Investigation of the Asymmetric Characteristics and Temperature Effects of CdZnTe Detectors

Benjamin W. Sturm, *Student Member, IEEE*, Zhong He, *Senior Member, IEEE*, Thomas H. Zurbuchen, and Patrick L. Koehn

***Abstract*—The results of our newest depth sensing coplanar grid CdZnTe detectors will be discussed. These detectors, which utilize the third-generation coplanar anode design, were fabricated by Baltic Scientific Instruments, Ltd., using crystals acquired from Yinnel Tech, Inc., having dimensions of 1.5 cm $\times$1.5 cm$\times$ 0.9 cm and 1.5 cm $\times$1.5 cm$\times$ 0.95 cm. Employing various compensation techniques, an energy resolution of about 1.7% full width at half maximum (FWHM) was achieved for 662-keV gamma rays. We observed that the spectral performance was highly dependent upon the biasing orientation of the detector. The $\mu_e\tau_e$ product for one of the crystals was measured and it was found to be a high value of 1.13×10^{-2} cm^2/V. A study of the spectroscopic performance of CdZnTe for reduced temperature operation was implemented and we observed degraded performance for temperatures below 0°C and a complete loss of spectral information at -30°C.**

***Index Terms*—CdZnTe detector, coplanar grid, depth sensing, gamma-ray spectroscopy.**

I. Introduction

CdZnTe has become a proven detection material with a high atomic number for good γ-ray stopping efficiency and a sufficiently large bandgap (1.7 eV) for room-temperature applications. The poor $\mu_h\tau_h$ product for this material makes it difficult to operate in a planar electrode configuration. However, the adverse effects of poor hole mobility can be ignored when utilizing in a single-polarity charge sensing mode. That is, by sensing the movement of electrons solely, the slow-moving holes will no longer act to degrade detector performance. In this way, the favorable properties of CdZnTe as a room temperature γ-ray detection device can be exploited, while mitigating the normally detrimental effect of poor hole mobility.

The method of single-polarity charge sensing in CdZnTe was first implemented by Luke by way of the coplanar grid electrodes [1]. These electrodes consist of two grids that when operated in a subtraction mode, produce a net signal that depends only on the movement of charge carriers very near to the grids. Thus, when operated as anodes, the coplanar grid electrodes will have a signal proportional to the number of electrons collected. Due to the effects of electron trapping, however, the number of electrons collected will be dependent on the depth of the γ-ray interaction, resulting in a depth-dependent subtracted signal. In order to circumvent this dependency, Luke introduced a means to compensate for the effects of electron trapping. This was done by applying a relative gain to one of the coplanar anode signals, introducing an artificial charge induction component to the subtracted signal that grows with increasing distance from the anodes. By selecting the optimal relative gain and assuming good material uniformity throughout the whole crystal, near-ideal electron trapping compensation can result.

Shortly after Luke's finding, He *et al.* proposed a method using depth sensing to correct for electron trapping [2], [3]. By taking the ratio of the cathode and subtracted signals, the interaction depth of the γ-ray event can be determined. This ability to sense the depth of the γ-ray interaction provides us the additional capability to obtain spectra as a function of interaction depth. Hence, by plotting the spectrum at each depth, we can clearly observe the shifting of the photopeak amplitude due to electron trapping. In addition, by aligning the photopeaks of each spectrum in our spectral analysis program such that the peak centroid values coincide, we can obtain the depth-corrected spectrum with improved energy resolution. This method has the advantage of achieving compensation for any depth-dependent variation in electron trapping or material properties. The depth sensing method allows us to obtain a one–dimensional (1-D) spectral mapping of the detector, giving us additional knowledge of detector material properties and charge induction uniformity.

The design of the coplanar electrodes has undergone a number of modifications since conception. The original design, named generation 1, consisted of two simple coplanar grid electrodes. He *et al.* observed significant energy resolution degradation near the coplanar anodes, which was later attributed to the weighting potential asymmetric effect [4]. As a means to reduce this effect, the generation 2 design was proposed, which involves a boundary electrode surrounding the two interior coplanar anodes. The boundary electrode helps to both balance the weighting potential symmetry as well as absorb excess leakage current from the sides of the detector which allows for higher biasing and thus improved charge collection efficiency. With the addition of the boundary electrode, a significant improvement in energy resolution near the coplanar anodes was observed. Although the generation 2 design was superior to the previous configuration, He *et al.* still recognized that the weighting potential symmetry could be improved further. This improvement can be achieved by adjusting the widths of the two outermost strips and three outermost gaps in order to minimize the difference in the coplanar grid weighting potentials. This new design was labeled generation 3 and again significantly better resolution near the coplanar anodes was observed in

Manuscript received November 16, 2004; revised April 12, 2005. This work was supported in part by NASA PIDDP Program, Award Reference 856426, and the U.S. Department of Energy under Grant DE-FG03-01NN20122.

The authors are with The University of Michigan, Ann Arbor, MI 48109-2104 USA (e-mail: bwsturm@umich.edu; hezhong@umich.edu; thomasz@umich.edu; koehn@umich.edu).

Digital Object Identifier 10.1109/TNS.2005.856728

comparison to the generation 2 design. In fact, utilizing eV Products detectors with our generation 3 design, better energy resolution was observed near the coplanar anode side than on the cathode side, a testament to the uniformity of the weighting potentials near the anodes [1].

This paper provides an evaluation of two detectors obtained using Yinnel Tech, Inc., crystals which are grown by way of the Modified Vertical Bridgman (MVB) technique [2], [5]. Crystals grown by the MVB method are stated to have higher single crystal yield than those grown using the high-pressure Bridgman method. The crystals were fabricated into detectors by Baltic Scientific Instruments, Inc. (BSI), using the generation 3 coplanar grid design [3]. The final detector sizes were 1.5 cm $\times$1.5 cm$\times$ 0.9 cm and 1.5 cm $\times$1.5 cm$\times$ 0.95 cm.

II. Methods of the Study

The focus of this study was to evaluate the spectroscopic performance of detectors composed of CdZnTe crystals grown by the MVB method. We accomplished this by first designing the coplanar grid electrodes utilizing the generation 3 design concept. Then, we took great care in specifying how the detector was to be fabricated. Finally, a series of measurements were performed to evaluate the performance of the detector for γ-ray detection. These measurements were taken both for room-temperature operation as well as for reduced temperature environments.

A. Considerations in Detector Design and Fabrication

The design of the coplanar grid electrodes was carried out using the three–dimensional (3-D) electrostatic finite-element analysis software package Maxwell[4] . This package can easily simulate the weighting potential field for any electrode of interest. Because our goal is to achieve uniform response independent of the γ-ray interaction location, we sought to minimize the difference of the weighting potentials for the coplanar anodes. As a means of comparing design simulations, we used the following figure of merit (FOM) value:

$$\text{FOM} = \overline{|W1 - W2|} \tag{1}$$

where $W1$ and $W2$ are the weighting potentials for either coplanar grid anode at some specified point within the simulation mesh. Smaller FOM values indicate better weighting potential uniformity. In addition to the weighting potential symmetry, it is also very important to keep in mind the effects of detector capacitance, which is related to the amount of electronic noise observed in the system. So, a balance between the detector capacitance and the FOM value must be met in order to achieve the optimal detector performance. We adapted our design from a previous detector design having a strip width of 300 μm and gap width of 150 μm in the central region of the electrode surface. We then made adjustments to the outermost gaps and strips and simulated a variety of different designs to achieve what we believed to be nearly an optimal balance between the FOM and capacitance.

The coplanar electrodes have been fabricated on both sides of the detector to increase the chance for successful performance. To operate one side of the detector as a cathode, the three electrodes on that side are coupled together by connecting the corresponding signal wires together. The other side is then operated in the standard coplanar anode mode. With the advent of coplanar anodes on both sides of the detector we now have the added flexibility to select which side is to be operated as the anode and which side is to be operated as the cathode. This then assures us that the detector can be operated in a means to achieve the best performance.

B. Measurements at Room Temperature

To characterize the performance of the detectors at room temperature, we acquired gamma-ray spectra using either of the two electron-trapping compensation techniques. One technique is the relative gain method and the other technique is the depth-sensing method. With coplanar electrodes fabricated on either side of the detector (labeled side "A" and "B") we acquired spectra for both biasing configurations, that is with side "A" biased as the anode and side "B" biased as the cathode and *vice versa*. We also conducted $\mu_e\tau_e$ product calculations using the method for single-polarity charge-sensing devices [6]. In this method, we expose the detector to a low-energy γ-ray source on the cathode side such that the electron cloud will drift over the entire detector thickness. Then, we measure the photopeak centroid position for spectra acquired at two different bias voltages. The $\mu_e\tau_e$ product can be determined based on the photopeak shift observed at these two bias voltages.

C. Measurements for Varying Temperatures

There is wide-spread interest in the scientific community to characterize the performance of CdZnTe detectors for low-temperature environments such as those found on Mars. To accomplish this, we used a temperature chamber that could easily reach temperatures down to $-30\,^{\circ}$C. The detector box, which includes the detector, preamplifier electronics, and the subtraction circuit, was placed inside the chamber. The biasing and signal cables were fed through a hole on the side of the chamber. Care was taken to reduce the concentration of water vapor surrounding the detector box which could possibly lead to water condensation on the electronics. This was done by supplying a flow of dry N_2 gas into the chamber as well as placing containers of desiccant inside the chamber. Energy spectra were taken during the cooling cycle for temperatures of 20 °C, 10 °C, 5 °C, -5 °C, -10 °C, -20 °C, and -30 °C. Spectra were also taken during the warming cycle. In addition, we conducted measurements of the $\mu_e\tau_e$ product for each temperature setting. An independent set of measurements were performed, which were taken at a later time, to characterize the μ_e value at each temperature setting.

III. Performance at Room Temperature

We began by testing the Yinnel Tech/BSI CZT2-4-2 detector because it was found by BSI to be the better of the two detectors.

[1]eV Products, Saxonburg, PA, USA.

[2]Yinnel Tech. Inc., South Bend, IN, USA.

[3]BSI Ltd., Riga, Latvia

[4]Maxwell 3D, Ansoft, Pittsburgh, PA, USA.

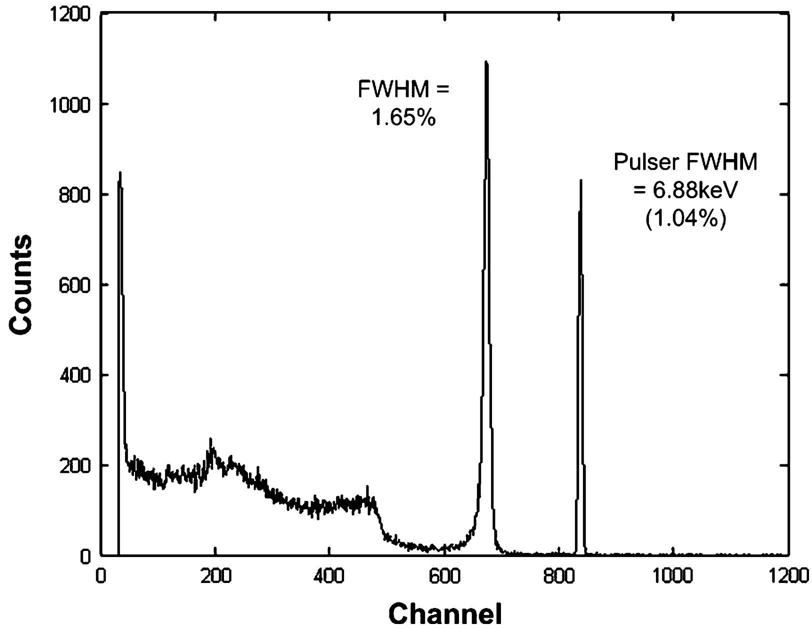

Fig. 1. 662-keV γ-ray energy spectrum for the CZT2-4-2 detector using the relative gain compensation method. Results in the range of 1.65% to 1.70% were consistently achieved.

With a bias of -1200 V supplied to the cathode, -40 V supplied to the noncollecting anode, and with the collecting anode and boundary electrode set to ground, we achieved a full width at half maximum (FWHM) at 662 keV of 1.65% using the relative gain method for electron trapping compensation. The pulse height spectrum for this measurement is given in Fig. 1. The spectrum in Fig. 1 was acquired with side "A" biased as the anode. By reversing the biasing polarity such that side "B" is biased as the anode, we achieved an FWHM at 662 keV of 6.8% using the relative gain method, which clearly indicates a severe degradation in performance.

As was previously described, the depth-sensing method for electron trapping compensation allows us to obtain energy spectra as a function of interaction depth. For the condition in which side "A" is biased as the anode, Fig. 2(a) shows both the uncorrected γ-ray spectrum and depth corrected spectrum. Fig. 2(b) illustrates the depth dependency for energy resolution in the detector where larger depth indices indicate increasing distance from the anodes. We find that the resolution remains fairly constant in the bulk of the detector, but then degrades significantly near the coplanar anodes. This effect was surprising to us, because of what we had observed earlier on an eV Products detector using a similar generation 3 coplanar grid electrode design—namely, the effects of weighting potential asymmetry observed on the generation 2 detector were reduced on the generation 3 detector to the point where the best resolution obtained was very near to the coplanar grid anode [7]. With side "B" biased as the anode, we acquired the energy spectrum as shown in Fig. 3(a). In Fig. 3(b), we observe linearly degrading resolution as a function of increasing depth from the coplanar anodes. This indicates that the degradation of energy resolution is related to the drift distance of electrons, which seems to be a strong indication that this is due to a material bulk effect. However, the effect of a thin surface layer cannot be ruled out completely, since this could alter the electric field distribution in the bulk making the effect of charge trapping more severe.

A measurement of the CZT2-4-2 detector $\mu_e\tau_e$ product was carried out as described previously. With side "A" biased as the anode we measured a value of 1.13×10^{-2} cm^2/V. This value is high in comparison to traditional $\mu_e\tau_e$ values, which should help to explain the excellent performance achieved with this detector. With side "B" biased as the anode we measured a value of 8.83×10^{-3} cm^2/V. The uncertainty in this measurement is characterized by the depth resolution of the detector, which is $\sim$5%, so the difference in the $\mu_e\tau_e$ for opposite biasing polarities is significantly greater than the uncertainty. However, it must be stated that this calculation assumes a uniform electric field, which may not be the case if a surface layer were present that could substantially affect the electric field distribution. Still, this result provides some indication why we observed degraded performance with side "B" biased as the anode, since the detector characteristics were observed to be asymmetric.

Energy spectra were also taken with the Yinnel Tech/BSI CZT2-4-1 detector and very similar behavior was observed. The best resolution achieved for this detector was 1.86% at 662 keV. A summary of the energy resolution data for both detectors is given in Table I.

IV. Evaluation at Varying Temperature

The temperature study was carried out for both the eV Products detector MO2 2-2 square and the Yinnel Tech/BSI detector CZT2-4-2. Using the depth-sensing method for electron trapping compensation, we acquired energy spectra at each temperature setting. The results for the eV Products detector are displayed in Fig. 4 and that for the Yinnel Tech/BSI detector are displayed in Fig. 5. For the eV Products detector, we observed the best energy resolution at 5 °C of 2.1%. Below this temperature, continuously degrading energy resolution was observed

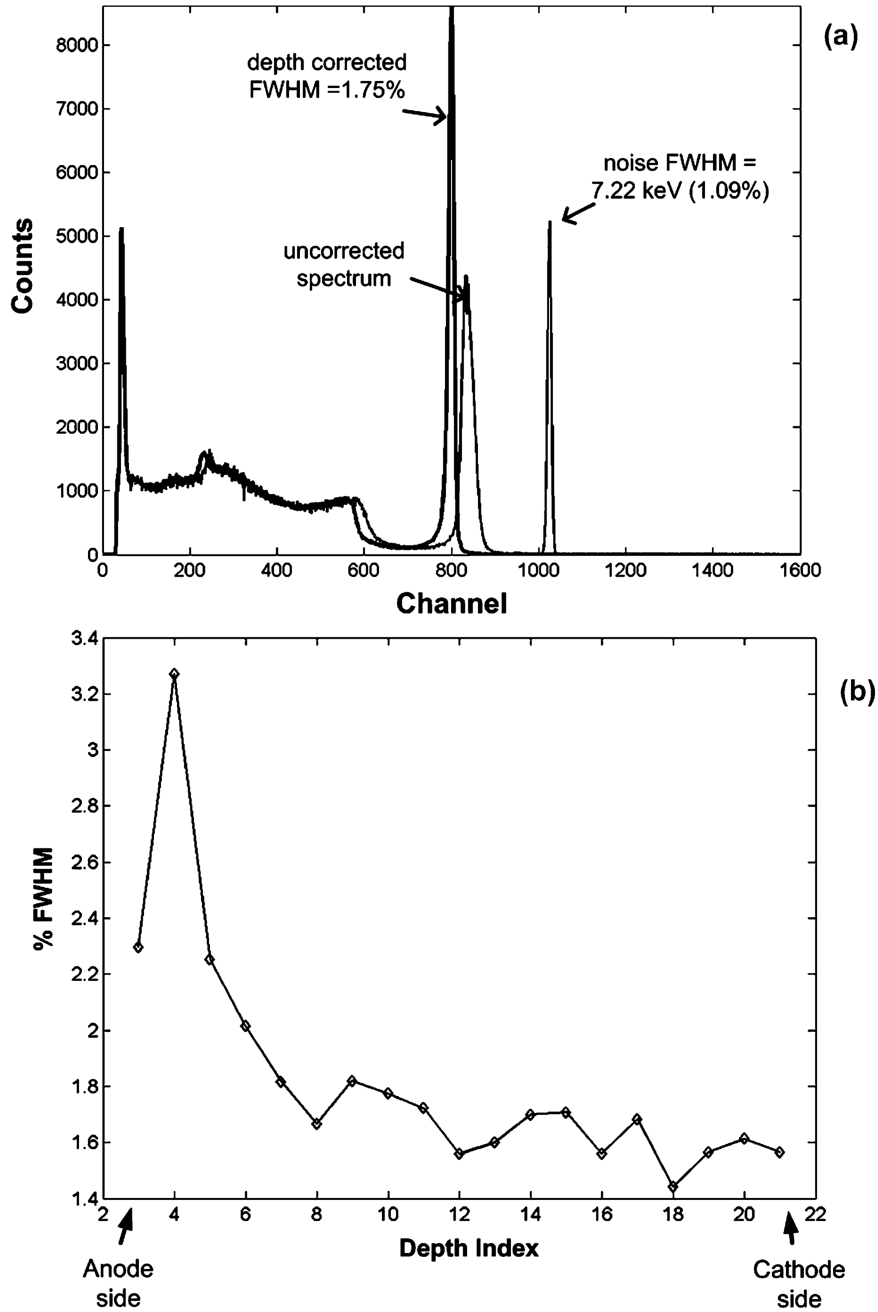

Fig. 2. (a) Energy spectrum for 662-keV γ-rays using the depth sensing method. (b) Resolution versus depth number where increasing depth indices indicate increasing distances from the anode side of the detector. This measurement was taken with side "A" biased as the anode and side "B" as the cathode.

TABLE I
ENERGY RESOLUTION DATA FOR BOTH YINNEL TECH/BSI DETECTORS USING THE DEPTH SENSING OR RELATIVE GAIN METHODS FOR ELECTRON TAPPING COMPENSATION AND WITH EITHER SIDE 'A' OR SIDE 'B' BIASED AS THE ANODE

Detector	Anode side	% FWHM with depth sensing	% FWHM with relative gain
CZT2-4-2	A	1.75%	1.65%
	B	8.3%	6.8%
CZT2-4-1	A	1.86%	1.99%
	B	8.3%	7.0%

down to −20 °C with a value of 5.5%. A complete loss of spectral information was observed at −30 °C. The electronic noise was determined by the pulser FWHM and it was found that the noise reduced as a function of decreasing temperature, even at −30 °C. For the Yinnel Tech/BSI detector, we observed the best energy resolution at 20 °C of 2.4%. The poorer energy resolution observed at room temperature (20 °C) during this study, in comparison to previous room-temperature measurements, was most likely a cause of the vibrational effects of the temperature chamber. Worsening spectral performance was observed as a function of decreasing temperature with a resolution of 7.0% at −20 °C. This detector also resulted in a breakdown in performance at −30 °C.

In addition to the spectral performance of the detectors, an evaluation of the detector $\mu_e\tau_e$ product as a function of temper-

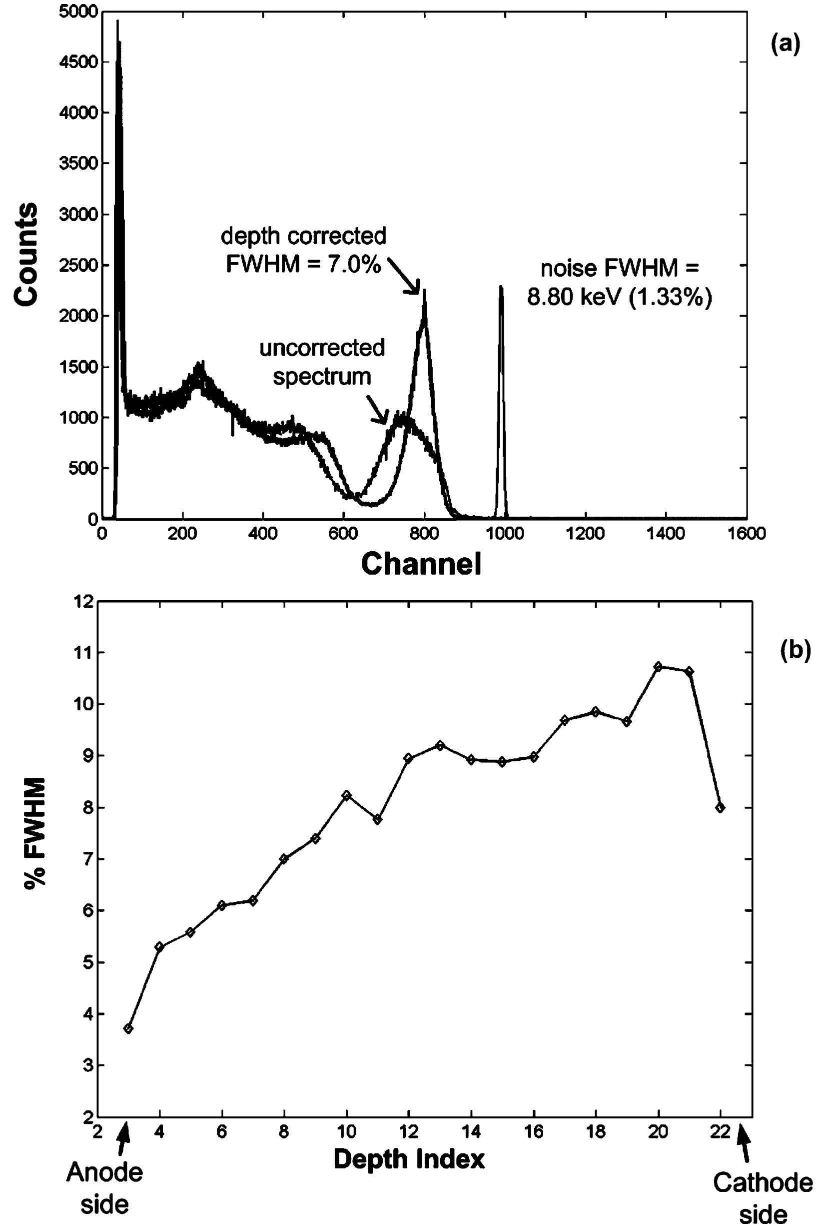

Fig. 3. (a) 662-keV spectrum and (b) resolution versus depth plot. In this measurement side "B" was biased as the anode and side "A" was biased as the cathode.

ature was carried out. In this method, we determined the $\mu_e\tau_e$ product values based on the photopeak shift observed between cathode side events and anode side events. This method is subject to some factors that could affect the precision of the measurement, including the possibility of a relative gain not exactly equal to 1. However, the relative change in the observed $\mu_e\tau_e$ should still be valid. Hence, we applied this method at all operating temperatures and normalized it to the known room temperature $\mu_e\tau_e$ product value. The data for both the eV Products detector and the Yinnel Tech/BSI detector is displayed in Fig. 6. For the eV Products detector we find that the $\mu_e\tau_e$ achieves its maximum value at 5 °C, where the energy resolution was observed to be the best, and then it falls off for decreasing temperature. For the Yinnel Tech/BSI detector we find that the $\mu_e\tau_e$ is the highest at 20 °C and higher than that of the eV Products detector. However, there is a sharp fall-off in this value with reduced temperature such that it falls well below the eV Products detector at -20 °C. These findings are in good agreement with the spectral behavior of the detectors as a function of temperature.

A separate set of measurements were carried out to determine the electron mobility value (μ_e) for the Yinnel Tech/BSI detector as a function of changing temperature. In this measurement, we acquired pulse waveforms for events originating near the cathode surface of the detector. By taking the rise time of such events we can determine the μ_e value. Twenty measurements were taken at each temperature setting to determine the uncertainty of the measured value. The results are shown in Fig. 7. We find that while cooling the detector the μ_e increases about 14% from 20 °C to -10 °C, which is what we would anticipate since the effect of reduced temperature would be a reduction in the crystalline lattice vibrations resulting in greater mobility because there would be fewer scatterings of the electron. However, we then observe a significant drop in the μ_e at -20 °C in addition to greater uncertainty in the measurement.

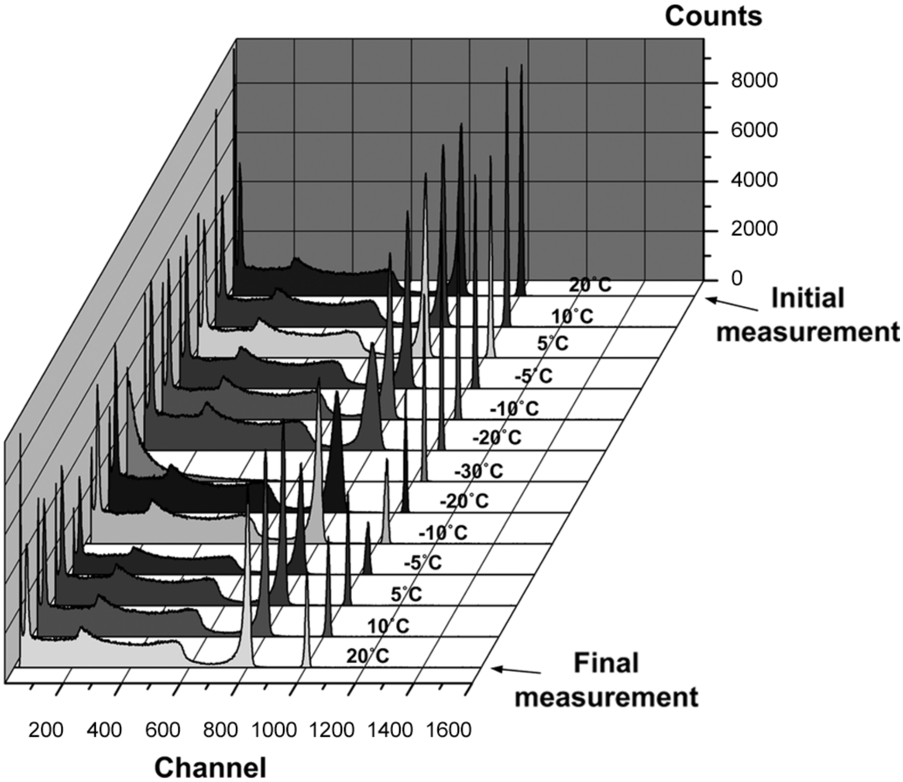

Fig. 4. Spectrum taken with the eV Products detector MO2 2-2 square for each temperature setting using a 662 keV γ-ray source. The spectrum at -30°C is characterized as a low energy continuum.

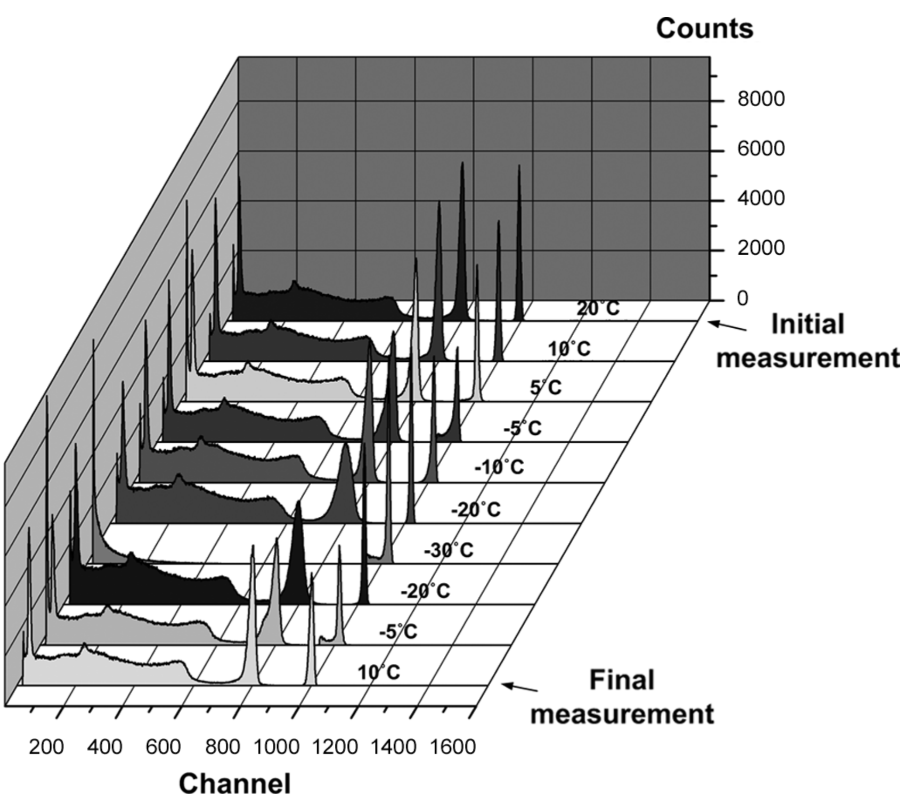

Fig. 5. Yinnel Tech/BSI CZT 2-4-2 detector spectrum taken at each temperature setting.

What we observed was that the pulse waveforms at -20 °C were either of two categories. The first category consisted of pulses that had a rounding-off feature during the signal rise, resulting in pulses of longer duration with typical rise times of ~ 1 μs. The second category consisted of normal pulse waveforms with typical rise times of ~ 0.85 μs. The distribution of

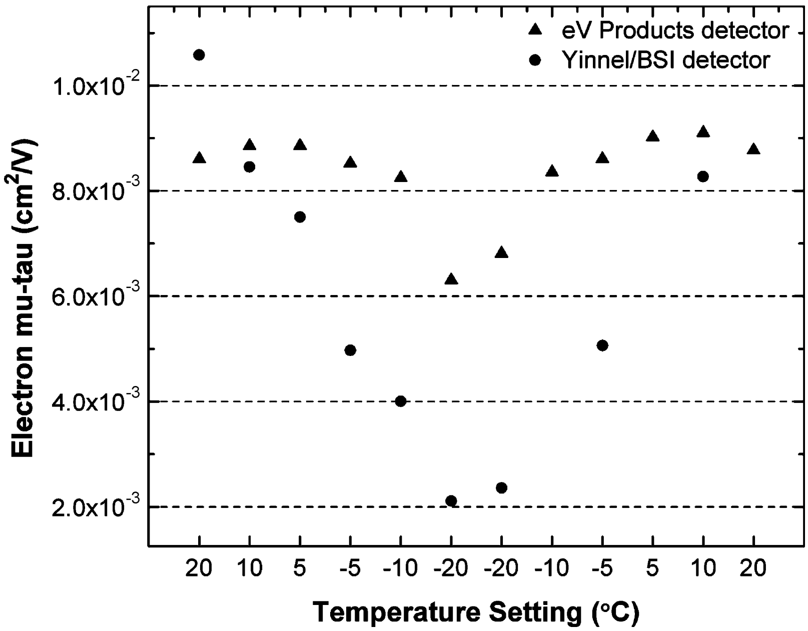

Fig. 6. $\mu_e\tau_e$ product values for two detectors as a function of operating temperature ($20\ ^\circ\mathrm{C} \rightarrow 10\ ^\circ\mathrm{C} \rightarrow 5\ ^\circ\mathrm{C} \rightarrow -5\ ^\circ\mathrm{C} \rightarrow -10\ ^\circ\mathrm{C} \rightarrow -20\ ^\circ\mathrm{C}$). Measurements were repeated at each temperature for the eV Products detector while heating. Only three measurements were performed for the Yinnel Tech detector during the heating cycle ($-20\ ^\circ\mathrm{C} \rightarrow -5\ ^\circ\mathrm{C} \rightarrow 10\ ^\circ\mathrm{C}$).

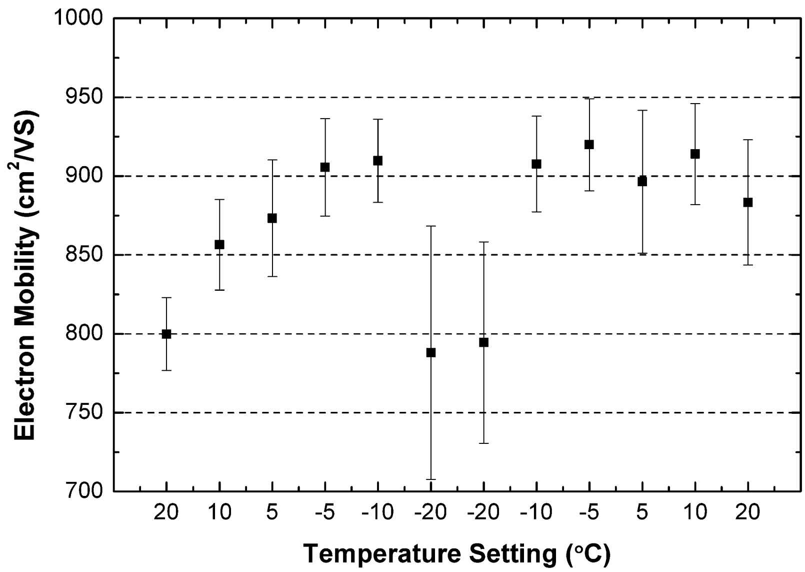

Fig. 7. BSI CZT2-4-2 detector μ_e values for changing temperature where the leftmost point is the initial measurement and the rightmost point is the final measurement.

waveforms at $-20\ ^\circ\mathrm{C}$ was divided among these two categories fairly evenly, which gave way to a large uncertainty in the mean of the μ_e value. During the heating cycle we observe a similar trend in the μ_e from $-20\ ^\circ\mathrm{C}$ to about $5\ ^\circ\mathrm{C}$. At $10\ ^\circ\mathrm{C}$ and $20\ ^\circ\mathrm{C}$ the μ_e remains fairly constant, which could either be a result of the error associated with the measurement or the possibility that the chamber temperature was not held long enough such that the detector did not fully assume the operating conditions.

The effect of poorer spectral performance for temperatures below $0\ ^\circ\mathrm{C}$ and a complete loss in spectral information at $-30\ ^\circ\mathrm{C}$ is not yet fully understood. Examining the BSI detector data we find that the $\mu_e\tau_e$ product reduces by a factor of $\sim$5 from $20\ ^\circ\mathrm{C}$ to $-20\ ^\circ\mathrm{C}$ and the μ_e increases only slightly over the same temperature range. Hence, the electron lifetime τ_e must also reduce by a factor of $\sim$5 over this temperature range. One possible theory to explain this observation is that the charge trapping levels become deeper with reduced temperature. That is, trapped charges are less likely to detrap, resulting in a shorter lifetime. Another clue to help us understand the physical effects occurring in CdZnTe at reduced temperature can be obtained from the pulse waveforms. At $-20\ ^\circ\mathrm{C}$, the previously mentioned first category pulse waveforms had a rounding-off effect in addition to longer rise times. This may be the result of longer electron detrapping times, since this would result in an elongated electron cloud giving way to the types of pulse waveforms we observed. The coplanar signal for events originating near the anode surface did not result in longer rise times at -20 °C since the electron drift distance would be reduced and hence would not be as affected by trapping and detrapping. At -30 °C, the anode pulses were much smaller in amplitude than what was observed for warmer temperature conditions. In many cases, the collecting and noncollecting anode signals were of the same polarity while the cathode signal was of the opposite polarity. This indicates to us that the electrons travel only a short distance within the bulk of the detector before becoming trapped.

V. Concluding Remarks

Two detectors composed of crystals grown by Yinnel Tech using the MVB technique were tested. Both detectors achieved excellent spectroscopic performance. The best energy resolution observed was 1.65% at 662 keV. The $\mu_e\tau_e$ product was measured for one of the crystals and it was found to be a high value of 1.13×10^{-2} cm^2/V. It was determined that the detector properties were asymmetric, such that the detector performance was highly dependent on the biasing orientation. We also found that the spectroscopic properties for two CdZnTe detectors using crystals grown with two different methods became worse at reduced temperatures. A complete loss of spectral information was observed at -30 °C, indicating that CdZnTe detectors are best operated at room temperature.

Acknowledgment

We would like to extend our appreciation to K. Cooper and D. Boprie of the Space Physics Research Laboratory for their help and support in setting up the temperature study experiment. We also extend our gratitude to J. Berry for his expert advice in the design of the read-out electronics.

References

[1] P. N. Luke, "Unipolar charge sensing with coplanar electrodes. Application to semiconductor devices," *IEEE Trans. Nucl. Sci.*, vol. 42, no. 4, pp. 207–213, Aug. 1995.

[2] Z. He, G. F. Knoll, D. K. Wehe, R. Rojeski, C. H. Mastrangelo, M. Hammig, C. Barrett, and A. Uritani, "1-D position sensitive single carrier semiconductor detectors," *Nucl. Instrum. and Methods in Phys. Res. A*, vol. 380, pp. 228–231, 1996.

[3] Z. He, G. F. Knoll, D. K. Wehe, and J. Miyamoto, "Position-sensitive single carrier CdZnTe detectors," *Nucl. Instrum. and Methods in Phys. Res. A*, vol. 388, pp. 180–185, 1997.

[4] Z. He, G. F. Knoll, D. K. Wehe, and Y. F. Du, "Coplanar grid patterns and their effect on energy resolution of CdZnTe detectors," *Nucl. Instrum. and Methods in Phys. Res. A*, vol. 411, pp. 107–113, 1998.

[5] L. Li, F. Lu, K. Shah, M. Squillante, L. Cirignano, W. Yao, R. W. Olson, P. Luke, Y. Nemirovsky, A. Burger, G. Wright, and R. B. James, "A new method for growing detector-grade cadmium zinc telluride crystals," in *2001 IEEE Nuclear Science Symp. Conf. Rec.*, vol. 4, 2001, pp. 2396–2400.

[6] Z. He, G. F. Knoll, and D. K. Wehe, "Direct measurement of product of the electron mobility and mean free drift time of CdZnTe semiconductors using position sensitive single polarity charge sensing detectors," *J. Appl. Phys.*, vol. 84, pp. 5566–5569, 1998.

[7] Z. He and B. W. Sturm, "Characteristics of depth sensing coplanar grid CdZnTe detectors," in *Proc 2003 IEEE Nuclear Science Symp, RTSD*, Portland, OR, 2003.